

CHAPTER 2

Infrared radiation and materials interaction: Active, passive, transparent, and opaque coatings

Charu Dwivedi^a, Priyanka Bamola^b, Bharti Singh^c, Himani Sharma^b

^aDepartment of Chemistry, School of Physical Sciences, Doon University, Dehradun, Uttarakhand, India

^bDepartment of Physics, School of Physical Sciences, Doon University, Dehradun, Uttarakhand, India

^cDepartment of Applied Physics, Delhi Technological University, Delhi, India

1 Introduction

A broad spectrum of wavelengths ranging from 295 to 2500 nm reaches in our environment as sun light, scientifically in forms of visible, UV (ultra violet), & IR (Infrared) (1–4). In IR regime, mainly three bands are considered: (1) short wave IR (SWIR); (2) mid-wave IR (MWIR) and (3) long wavelength IR (LWIR), depending on the wavelength, as shown in Fig. 2.1.

The origin of life on earth is mainly generated by the infrared radiation, and half of the sun's energy within the star spectrum falls on the IR radiation. IR, generally termed as thermal radiation, is the most important spectrum, which lies between visible and UV spectra. It has wavelengths from 0.74 to 100 μm .

William Herschel discovered IR radiation in 1800, when he found a set of an even warmer temperature measurements with the colors of visible spectrum (blue to red), using various thermometers. But Herschel could not explain the complete nature of IR radiation (5,6). During the second half of the 19th century, J.C. Maxwell contributed his four equations on electromagnetism, which unified the fundamental laws of electromagnetism (7). Later, Hertz proved these equations experimentally. By then, it was deduced that light and IR radiation have common nature and properties (7). Clearly, the idea of electromagnetism changed the whole perceptions of IR radiation. It supported further analysis and progressive approaches toward IR radiations. In 19th century, W. De. W. Abney and E.R. Festing mapped IR radiation in solar spectrum by their photographic emulsions and found a unique pattern. This laid a foundation of analyzing IR spectroscopy in modern science.

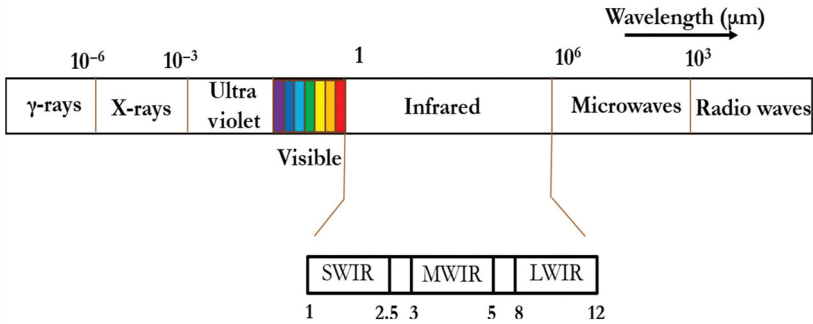


Figure 2.1 A diagram of electro magnetic spectrum and IR region.

In recent times, metals and nanostructures are being used in the study of IR radiation, which is important for its advancement in the modern science and technology, as well as in the overall development of mankind (4, 8, 9). IR radiation's silent presence in our surroundings does not affect its necessity for our existence on earth. Remote controlling devices, wireless connections, security systems, sensor development, optical fiber, thermal imaging, and various apparatus in hospitals daily use the technology of IR radiation (10–19). Analyzing the transferring and receiving patterns of IR radiation is the basic for these technologies. By using the absorption and emission spectra, we can determine the molecular structures. It is also helpful in determining the complex chemical mixture of molecules by both qualitative and quantitative analyses. Photovoltaic IR photo detectors based on thin-film materials (such as HgCdTe, InSb, InGaAs) have been widely used for earth observation, environment monitoring, and remote sensing (4).

In modern times, where the energy demand is increasing rapidly in our daily lives and industries, cost-effective and efficient medium is required, which also favors the environment. Solar energy is very important in this regard and it consists of energy in terms of UV, IR, visible and microwave regions.

The principle of absorption is applied generally to convert sunrays into various forms of usable energy, which are renewable. For example, in the absorption of UV radiation (43.0 eV), molecular ionization is used for the ejection of electrons beyond their molecular energy or transition from the ground state to upper electronic state within atoms in metal oxides (CuO, Cu₂O, TiO₂, etc.) (8, 13, 19). Semiconductors are generally used for the absorption of visible light (1.7–3.0 eV) to generate electricity by photovoltaic devices (4, 8). The absorption excites electron from the valence

bond to conduction band due to heat and impurities of the semiconductor (8,15,20,21). Now, the external circuit can produce electricity or can also be transferred to the photochemical cells for inducing reduction/oxidation (20,21). Normally, the absorption of IR radiation requires transitions from the ground state to excited states of molecular vibrations, which finally produce energy in the form of heat (21). Metals with high thermal conductivity can absorb or reflect IR radiation quickly as the quantum states of their vibrations lie within this region, although most metals reflect almost all IR radiation (18,21). Highly efficient thermal detection devices can be realized by increasing the IR absorbing capability (18).

2 Light reflection mechanism of IR radiations with metals and nanostructures

When a metal sample is exposed in direct sunlight, three phenomena can occur, namely reflection, transmission, and absorption (22). Reflection is of two types: mirror like reflection' (specular reflection) and diffuse reflection. Mirror-like reflection is more significant for optically smooth and highly absorbing sample surfaces. On the other end, diffuse reflection occurs when incident radiation penetrates into the powder and is further mirrored by the grain boundaries of the particle. In the diffuse reflections, particle size is most important, as the particle size decreases, the number of reflections at the grain boundaries will increase (8). As a result, the depth of penetration of incident light decreases, which leads to a decrease in absorption and an increase in reflectance.

Absorption of light is the excitation of an electron from one bonding state to higher bonding states (9). An interesting fact is that all types of light wavelengths cannot generate energy transitions (due to energy differences), and a specific wavelength is required for the process of absorption of light. For example, the wavelength between 400 and 700 nm is necessary to motivate electronic transitions (23,24). Anything higher than this wavelength (>700 nm) is not enough to generate power. Sun also has a wavelength of 1500 nm, which is ineffective for causing any electronic transition. Thus, the wavelength of 1500 nm beam will not be observed and when further being mirrored and scattered, it leads to the diffused reflection of NIR light (9). Although, there is no methodology for predicting the IR reflectivity of chemical and inorganic compounds (9).

Metals are opaque at IR wavelengths. This is because metals are characterized by their large concentrations of free electrons, which is the property

that gives them their highly reflective nature (25). Reflective metals can be pure metals (such as Au, Ti, Cu, Al, and Ag), metals with surface coatings (AgS on Ag and AlO(OH) on Al), and multiple-layered structures: TiO₂/Au, silicon powder, metal-coated particles, etc. (8,9). Coated metals have a decreased reflection factor corresponding to visual light. For example, the coating outside of the metal, which can be considered as a metal oxide, can absorb visual light, whereas the IR light of a longer wavelength passes through the coating and can be reflected by the underlying metal (26). These multilayered structures are designed to minimize the reflection of visual light whereas giving a high reflection of IR light (27).

High reflective pure metals such as Ag, Au, Cu, and Al are continuously being used in the visible and infrared spectral region (28). Material's reflectivity can be derived from the basic optics.

$$R = |1 - \hat{n}/1 + \hat{n}|^2 = (1 - n)^2 + k^2 / (1 + n)^2 + k^2 = 1 - 4n / (1 + n)^2 + k^2 \quad (2.1)$$

where R , reflectivity of Light at normal incidence; \hat{n} , Complex refractive index; n , real part of refractive index; k , extinction coefficient.

In the near infrared region if $n \ll k$, we can derive the following expressions:

$$k \approx \sqrt{\mu c^2 \tau / \rho (1 + \omega^2 \tau^2)} \quad (2.2)$$

$$n \approx 1 / 2\omega \sqrt{\mu c^2 / \rho \tau (1 + \omega^2 \tau^2)} \quad (2.3)$$

and

$$R \approx 1 - 4n / k^2 \quad (2.4)$$

where μ , magnetic permeability; c , speed of light; ρ , electrical resistivity; ω , angular frequency; τ , mean free time between charge carrier's collisions.

Reflectivity is then obtained by inserting Eqs. (2.2) and (2.3) into Eq. (2.4).

$$R \approx 1 - \sqrt{4 / \mu} \quad c^{-1} \tau^{-1/2} \rho^{1/2} \quad (2.5)$$

Table 2.1 Comparison of the electrical resistivity and light reflectivity of pure Ag, Cu, Al, Mg crystalline films, several AgMgAl, AgCuMgAl, AgCuMg, and ZrCu thin-film coatings on glass substrate (all compositions are given in atomic percent) (28).

	Electric resistivity ρ, n^{**m}	Light reflectivity R , at 1000 nm
Ag	16	0.98
Cu	17	0.97
Al	27	0.94
Mg	45	0.92
Ag ₃₅ Cu ₃₅ Mg ₃₀ (crystalline)	189	0.98
Ag ₇₆ Mg ₁₇ Al ₇ (crystalline)	230	0.95
Ag ₇₃ Mg ₁₇ Al ₁₀ (crystalline)	286	0.92
Ag ₆₀ Mg ₂₇ Al ₁₃ (crystalline)	304	0.91
Ag ₃₀ Mg ₄₅ Al ₂₅ (amorphous)	1032	0.79
Ag ₃₀ Cu ₃₀ Mg ₁₅ Al ₂₅ (amorphous)	1120	0.77
Ag ₄₅ Mg ₃₇ Al ₁₈ (amorphous)	1178	0.77
Zr ₅₀ Cu ₅₀ (amorphous)	2975	0.60

Magnetic permeability has negligible effect on reflectivity because it is essentially constant for ferromagnetic metals. It is observed in Eq. (2.5) that a material with low ρ and high τ would exhibit high reflectivity.

Hu et al. investigated electrical resistivity and optical reflectivity, where they prepared a series of multicomponent AgMgAl alloys on glass substrate by sputtering technique (28). Table 2.1 shows that reflectivity is a function of resistivity for multi component AgMgAl alloys and it scales with the square root of electrical resistivity, which can be explained by the classical reflection theory given by Eq. (2.5).

3 Factors affecting infrared reflectivity

IR reflectivity basically depends on the relative ratio of the particles, neighboring medium, and distribution of particles within the coating, concentration, particle's size, and wavelength of the incident light (29). Coating thickness is an important criterion that affects film reflection factor. Higher coating thickness ends up with higher reflection factor due to the upper range of nanoparticles on the substrate for reflective (29). Recently, the optical properties of nanocrystalline and connected materials are becoming theoretical and experimental interest. Nanocrystalline materials possess fascinating optical properties like increased band gap and increased light intensity. Among the nanocrystalline materials, metal compound nanoparticles belong

to a stimulating category of compounds (30). Metal compound nanocrystals will be ready in distinctive shapes and they exhibit remarkably totally different chemical properties compared to macrocrystals. The particle size of a compound will have an effect on its color that successively will have an effect on its reflection factor properties. Moreover, metal compound nanoparticles possess high surface areas, which make them very helpful for a range of applications as well as coatings (31). The present oxides of the metallic element at air pressure exhibit three phases: anatase, brookite, and mineral (8). The mineral part is thermodynamically the foremost stable and possesses the best density with a compact atomic structure. TiO_2 within the mineral part is essentially used in reflective coatings attributable to its effective lightweight scattering properties. Recently, it has been found that the mineral part nanoparticles have higher absorption within the visible region compared to those of the anatase part (32,33). Coatings containing even bit of mineral part TiO_2 particles replicate nearly the complete visible spectra. Reflective coatings of TiO_2 are applied in business optical merchandise like optical fibers, integration spheres, luminaries, reflective panels, and optical device cavity mirrors (9). Studies on the reflection factor of TiO_2 particles are the topic of serious analysis for several decades as their applications need high photo stability and high reflection efficiency. The improvement in the photo stability of mineral part of TiO_2 while maintaining reflection factor at an equivalent time has been a difficult subject.

Doping TiO_2 with Al, Li, and K is one among the better ways to enhance the reflection factor of TiO_2 particles (34). It creates defects within the TiO_2 space lattice and introduces traps for electrons and holes. This will stop the migration of electrons and holes toward the surface of TiO_2 . The impact of Al doping on the reflective properties of TiO_2 nanoparticles and synthesized exploitation of the sol-gel technique has been investigated in 2013 by Kumar et al. (34) It has been shown that with Al doping, the transition temperature for anatase to mineral part was increased; but no change in morphology was observed. TiO_2 nanoparticles doped with 0.1% Al showed high photo stability with no amendment in reflection factor (34). The coating with Al-doped TiO_2 nanoparticles has been applied on a plastic substrate with totally different coating thicknesses to design lightweight reflectors. These reflectors are found to possess diffuse reflection factor of 98.17%–98.29% for 0.25-mm-thick coatings. In 2010, A. Ranade were synthesized niobium (Nb)-doped TiO_2 films using several different techniques (35). Nb was originally chosen because of the dopant material attributable to its similarity in atomic radius to Ti^{4+} and also the valence state it prefers (35). Zinc

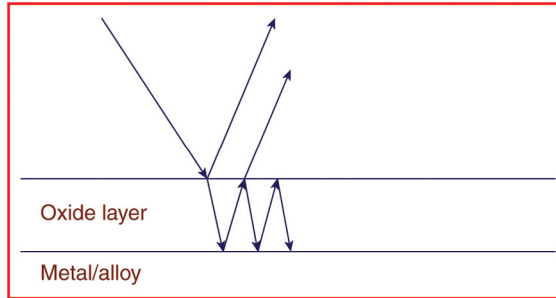


Figure 2.2 An oxidized surface capturing the light inside the oxide layer, which may further enhance absorption (25).

oxide nanoparticles coated with metallic element increased the reflective performance. In comparison to the uncoated material, the coated nanoparticles possess ten percent more reflection factor in 400–800 nm (36). Fe_2O_3 , Cr_2O_3 , Sb_2O_3 , and ZrO_2 are other metal oxides having high refractive indices; to achieve high reflectance over a wide spectral range, more than one type of metal oxides can be used (37). Metals also naturally have a layer (or several layers) of oxides on the surface. The chemical and optical properties of the oxides can often be very different from the properties of the metal or alloy underneath (25). In Fig. 2.2, the oxide layer enhances the absorption by capturing the light (25).

Cadmium stannate (Cd_2SnO_4) is one among the foremost clear, heat reflective semiconductors. Cadmium stannate films on an oxide plate replicate infrared at 1.5 μm film thickness (38). These films provide eighty percent reflectivity at 2 μm film thickness and 90% reflectivity at 6 μm thickness. These properties build metallic element stannate films extremely appropriate for greenhouse window applications (38). Another study describes the employment of colored metallic pigments like mica flakes and aluminum for better infrared reflectivity (26). According to the study, color has been incorporated on the metallic surfaces in such a way that it does not interfere with the ability of metallic pigments to control infrared reflectivity (26).

4 Regulating infrared radiation using inorganic and organic reflective materials

4.1 IR regulating inorganic materials

The IR reflective material either reflects in IR region or transmits the light. The reflectance of any material is usually due to specular reflectance and

diffuse reflectance. Specular reflectance is associated with the visual brightness or mirror quality of a surface and it depends on the surface smoothness (39). As the roughness of surface increases, the multiple reflections occur in the material and the component of diffuse reflectance increases and surface appears dull or matte finished. Diffuse reflectance of a material is determined by the particle shape, size, and distribution of the material (40–42). The total reflectivity of reflective coating is also decided by the chemical composition and refractive index of the pigment and the binder material (43). If the refractive index of the pigment is similar to that of the binder refractive index in the IR region, it will be transparent to the IR radiation (43). An ideal reflective material should have not only high reflection but also low emissivity and good corrosion resistance.

Over the years, different inorganic and organic materials are being investigated for their applicability as IR reflective materials. Inorganic IR regulating materials are the most commercialized ones due to their ease of processing and high stability. Inorganic IR reflecting materials include transition metals such as Ag, Au, Cu, Al, Ti, and Rh, the nitrides, boride and carbides of Ti, Zr, Hf, V, Nb, Ta, Cr, Mo, and W, metal oxides of Cr, Fe, Ti, Ce, and Mg (44–47).

Transition metal-based IR reflective materials have reported to have highest reflectivity in the IR band range and variable absorption in the visible region. The advantage of metallic coating lies in their broadband reflectivity and high tolerance to thickness variations. Reflectivity of silver is highest among all other materials and it makes Ag the most popular choice for commercial applications (48–50). Silver coating can be used as a transparent window for visible light and reflective surface for IR radiation at the same time. The composite formation with silver and nanocrystalline silver can be processed into composite material by using metal oxide as a base and top layer (51). This process reduces the metallic glare of the silver without significant reduction in its reflectivity. The metal oxide layer also provides scratch and corrosion resistance to the reflective layer. The reflectivity of other coinage metals such as copper and gold is also comparable to silver, but oxidizing tendency of copper and high cost of gold makes them less popular choice of reflective materials (52,53). Dalpati et al. have demonstrated fabrication and application of $\text{TiO}_2/\text{Cu}/\text{TiO}_2$ heat reflector coating for use in heat regulating smart windows. They observed that on annealing the reflector film, the crystal quality of the TiO_2 improved and its IR reflectance is also increased up to 85% at 1200 nm (Fig. 2.3) (54). Aluminum is another transition metal, which is used extensively as reflecting material,

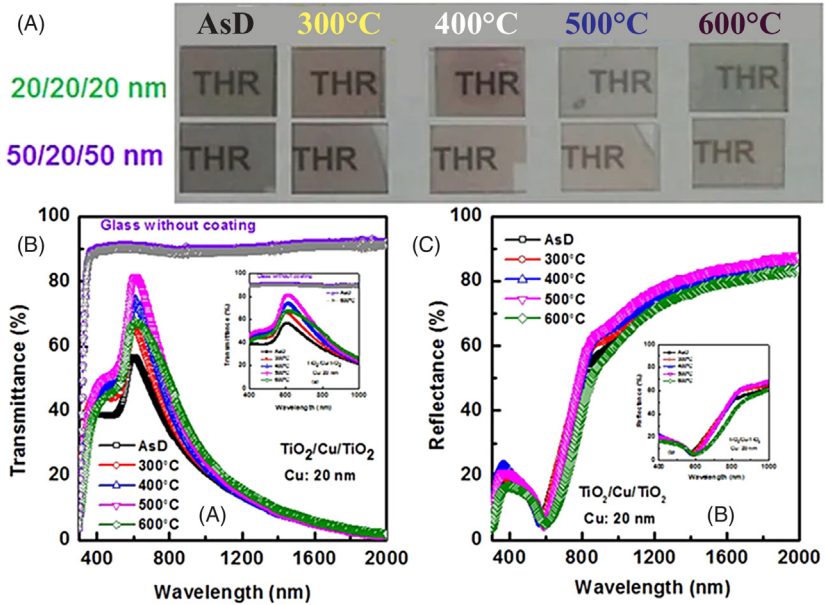


Figure 2.3 (A) Demonstration of TiO₂/Cu/TiO₂ heat reflector on glass substrate after thermal treatment (B) transmittance spectra and (C) reflectance spectra of TiO₂/Cu/TiO₂ thermal heat reflection with Cu layer thickness of 20 nm top TiO₂ layer thickness of 25 nm (C) *inset* of (B, C) show clear variation of heat reflector properties in the visible range and NIR region. Transmittance spectra of plain glass with and without thermal at 600 are also compared.

especially in the applications, which require broad spectral range of reflection (55). Aluminum is used as reflective surface in telescope mirrors and as parabolic or curved mirror in flat solar concentrators, but it is prone to weathering, which decreases its specular reflectance. The high IR reflectivity of metal-based coatings is due to the abundance of free electrons. But this also makes them susceptible toward easy wear and tear and corrosion.

The durability of the metallic coating can be enhanced by making its hybrid with a transparent protective coating. The coating materials are usually other transition metals or metal oxides such as TiO₂ and SiO₂. These materials are applied to protect the front surface of the reflective metal by dip coating, sol-gel thin coating, PVD, CVD or sputtering, electro or electroless plating (56). The efficiency of the processes varies with the choice of protective coating used and the method of coating. The optical properties of metal-based coating depend upon nucleation and growth phenomena and the impurities. The optical properties of metal and metal oxide coatings

are also significantly directed by the chemical composition, stoichiometry, and defects along with crystallinity and crystal structure. Therefore, various techniques for metal and metal oxide film deposition techniques are being developed globally. It has been observed that even the slight variation in the deposition technique or variation in the composition of the chemicals used can alter the optical and physical properties of the reflective coating (57,58). CVD, PVD, ion, and magnetron sputtering and electroplating are the most commonly employed deposition techniques (59,60). CVD and PVD techniques result in uniform and thin reflective layer but the setup for these techniques is expensive and processing on large surface area with these techniques is a challenge. There are not many options available for finding thermally stable precursors for use in CVD techniques. At higher temperatures, most of the metals tend to form their respective oxides, which create defects and impurities in the reflective coatings. The major drawback of electroplating is that it results in the films of thickness 50 nm or higher; additionally, the substrate is also required to be conducting surface.

Metal oxides and sulfides-based IR reflective materials are mostly used in paints, pigments, and camouflage materials (42,45). These materials show some absorption in visible band and emit rest of the visible radiation. The radiations from the visible band, which are emitted by these pigments, correspond to their color. For use in painting materials, these reflective materials are synthesized in the form of fine crystalline powder, which not only impart the paint its color and reflective property but also help in regulating viscosity of the entire formulation. The industrial production of metal oxide and sulfide nanocrystalline is relatively a cost-effective process. The oxides and sulfides of Ti, Fe, and Mn are usually doped with metals such as Fe, Cd, Ni, Sb, Zn, Cr, Bi, Cu, and Y to adjust the response of the host material towards radiations (61–63). Kalbunde et al. have investigated the effect of the size of the nanocrystalline metal oxide on the percentage reflectivity of various metal oxides. It is observed that the reflectivity of the metal oxide decreases with the increase in the crystalline size (Table 2.2) (45).

The IR radiations can also be regulated by doping the reflective coating with other transition metal ions. In this process, the amount of the dopant is required to be controlled as excess dopant could decrease the band gap of the native coating material and make it more absorptive in the IR region. Shi and coworkers investigated the effect of dopant on the reflectivity of the aluminum phosphate reflective coating. They observed that on Fe^{3+} doping, there was a significant decrease in the band gap from 5.98 to 3.60 eV resulting in the absorption of more NIR and decrease in the reflectance (64). The

Table 2.2 NIR reflectance properties of nanocrystalline metal oxides and macrocrystalline metal oxides.

Metal oxide	R% at 810 nm	Mean particle aggregate size (μm)	Average crystalline size (nm)	Surface area (m^2/g)
NC-CeO ₂	110	61.6	≤ 7	≥ 50
MC-CeO ₂	92	95	55	6
NC-Al ₂ O ₃	102	2.6	Amorphous	≥ 275
MC-Al ₂ O ₃	92	2.6	70	68
NC-TiO ₂	108	14.5	Amorphous	≥ 500
MC-TiO ₂	98	16.4	79	8
NC-MgO-I	109	4.2	8	≥ 230
N-MgO-II	105	7.8	≤ 4	≥ 600
MC-MgO	103	2.4	23	45

MC, macrocrystalline; NC, nanocrystalline; R%, the relative reflectivity was calculated compared to bulk materials.

reflectivity of the surface could also be increased using a combination of dopants. Yang and coworkers have synthesized Fe/N-doped MgTiO₃ as IR reflective pigment by sol gel method. The doping with Fe/N not only made the MgTiO₃ pigment more IR reflective but also imparted it a dark red blue color (65). In another work, George and coworkers have synthesized yttrium molybdenum oxide-based IR reflective material using silicone and praseodymium as dopants. The authors have reported that the color, hue, and the IR reflectivity of the pigment are regulated by change in the stoichiometric addition of the dopant material (66). The mechanism by which the dopant affects the IR reflectivity is different in the case of Si and Pr. In silicon-doped material, an addition phase $\alpha\text{-Y}_2\text{Si}_2\text{O}_7$ is formed, which increases the apparent concentration of Mo⁶⁺ ions in the crystal lattice; this results in decrease in the band gap from 2.60 to 2.45 eV. Whereas in the case of Pr, an additional energy level is created between O²⁻ and Mo⁶⁺ conduction bands due to the 4f electrons. This change in the energy levels causes the red shift in the absorption edge and decrease the band gap (66).

Other class of inorganic reflective material is metal carbides. Among these, silicon carbide has generated profound interest in aerospace industry due to its tunable IR reflectivity, high strength, moderate density, smaller thermal expansion coefficient, higher thermal conductivity, higher specific stiffness, and lower thermal deformation (67, 68). Metal nitrides and metal oxynitrides are being explored as IR regulating materials for solar applications. The advantages of these materials such as AlN, TiN, and TiAlN and

their complex nitrides lie in the fact that they are highly heat resistant, abrasive, and oxidation resistant, and have broad spectral selectivity (69,70). The production of these films/coatings can be achieved by DC magnetron sputtering or PVD techniques (25). The quasi-covalent bond formed due to hybridization between p and d orbitals makes the nitrides, borides, and carbides chemical-resistant, hard, and abrasion-resistant, and the unbound d electron in the transition metal imparts them metal like electrical properties. Therefore, a number of reflective and antireflective coatings are being developed for solar and electro optical applications.

4.2 NIR regulating organic materials

IR regulating organic materials are rare. The difference in the refractive indices of the organic materials is generally too low and a multilayer system is required to achieve significant IR reflection. The durability of these materials is not as good as that of the inorganic counterparts. However, the organic materials have found wide spread applications as a base material or one of the coatings in multilayered IR regulating surface. Organic pigments are also used in textile printing, inks, and paints. Examples of organic origin pigments include halogenated copper phthalocyanine, azo compounds, and a few perylene derivatives (71–73). Chlorophyll is naturally occurring IR reflective compound but due to its poor chemical stability, it cannot be used in commercial application. IR regulation is also reported by using liquid crystal (LC)-based switchable devices (74–77). These devices work on the fact that the orientation of the liquid crystals can be altered by applying an electric field, which also affects their transmittance. Liquid crystals are mainly of six types such as nematic, smectic, twisted nematic, cholesteric, guest–host, and ferroelectric (63,76). Among these, guest–host LCs-based switchable windows technology is commercialized since 1990 (63). Cholesterics liquid crystals are also employed for IR regulation for a variety of reflection-based technologies. The drawback with the use of regular cholesterics is their restricted d band width in the IR region (100 nm) but this problem can be solved by laminating a number of layers of this material during processing.

Khendelwal et al. have reported synthesis of organic-based IR reflectors for energy conservation. They have reported that energy consumption for temperature moderation in a building can be reduced by more than 12% by using a switchable IR reflector compared to a normal double glazing window and 9.3% compared to a static IR reflector (78). The authors have fabricated an electrically switchable dye (coumarin)-impregnated cholesteric

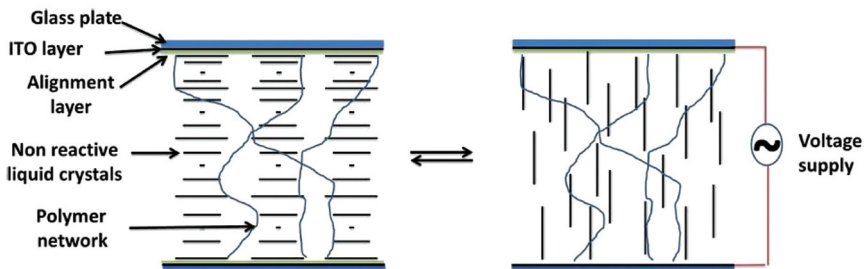


Figure 2.4 Schematic diagram shows the planar state (left) and homeotropic state on applying the electric voltage.

polymer gel-based coating. The schematic of this reflector is depicted in Fig. 2.4. Upon removing the electric voltage, orientation of the molecules reverts back to the original state in the presence of an alignment layer and polymer network.

A broadband IR reflector is also reported by Chen et al. by polymerizing LC cross-linker in the presence of azobenzene derivative (79). Nanoparticle-polymer composites are also used as IR regulating materials. The additional advantage of the polymer based reflective materials is ease of processing for commercial applications.

5 Active, passive, transparent, and opaque coating

In Sections 2.2 and 2.4, interaction of infrared radiation with metals and nanostructures, and its regulation using organic and inorganic materials were discussed in detail. This section endows details on the applicability of various IR coatings considering future energy supply and demands.

The wavelengths at which different optical coatings (thin films/nanostructures) perform varies over a large range. The selection of materials for coating depends on the application for which the particular system is being used under certain environmental conditions. The material coatings mainly are discussed in the context of coating for energy saving window applications. Cooling or heating strategy that keeps indoor comfort without electricity requirement could have a significant impact on global energy consumption. In order to cater to future energy supply and demands, and to slow down the insidious effects of global warming, energy-efficient buildings, vehicles, and windows are gaining importance (80,81). In that regard, a smart window is an energy proficient device that regulates heat according to weather conditions (summer/winter) at minimum demand of paid energy (air conditioning in summer) (82–84). Windows are most important

part of the building as they can be active, passive, opaque, and transparent at the same time. Many studies have been carried out in the context of smart windows (54,80,84–86).

Glass is used as a window on which no coating is performed. It allows the passage of visible light transmission as well as solar heat that increases the heating as well as cooling of the building structure. Materials coating is being performed on the glass to eliminate solar heat and reducing energy consumption. The materials are selected based upon their optical properties. They should be highly transparent in the visible region (380–760 nm) with high reflectance in the infrared spectral region (800–2500 nm) (80). The coating should be such that the long-wave radiation should not enter in the room from outdoors during summers, and should not escape from inside during winters, thus leading toward lower energy consumption during both the seasons (Fig. 2.5) (54,80,85). The spectral properties of such perfect windows are shown in Table 2.3. The energy serving approaches can be divided into two forms of active and passive coatings.

The active methods include improvement in heating and ventilation conditions. However, passive methods are related to the improvement in the properties and thermal performance of the building envelopes (84). The performance can be affected by adding thermal insulation to wall, using cool coatings on roofs and coated window glazing. These modifications lead to the change in the thermal properties and act as passive ways. These coatings can be applied by using various ways such as low-emission (low-e) coatings, thermos-chromic, aerogel, photochromic, electrochromic, gasochromic, and suspended particle and liquid crystal techniques.

Among various techniques mentioned, the low emissivity coatings are one of the potent techniques in regulating the long-wave thermal emission properties. Such low-e coatings aspire to allow the visible light pass through and block the IR and UV wavelengths and solve the purpose (87). There are various material coatings that are carried out on the glass to form the smart windows. Few of them are discussed in the 2.5.1 and 2.5.2 sections.

5.1 Dielectric/metal/dielectric coatings

In dielectric/metal/dielectric-based structures, dielectrics are made from metal oxides such as TiO_2 , SnO_2 , ZnO , HfO_2 , Cu_2O , and ZrO_2 whereas, the metal component typically comprises of silver (Ag), Au (gold), copper (Cu), and nitride-based materials (87). The D-M-ubD-based multilayered coatings on glass substrates serve that purpose for energy saving, as shown in Fig. 2.6. The thin metal layer is used for IR reflection and dielectric layers

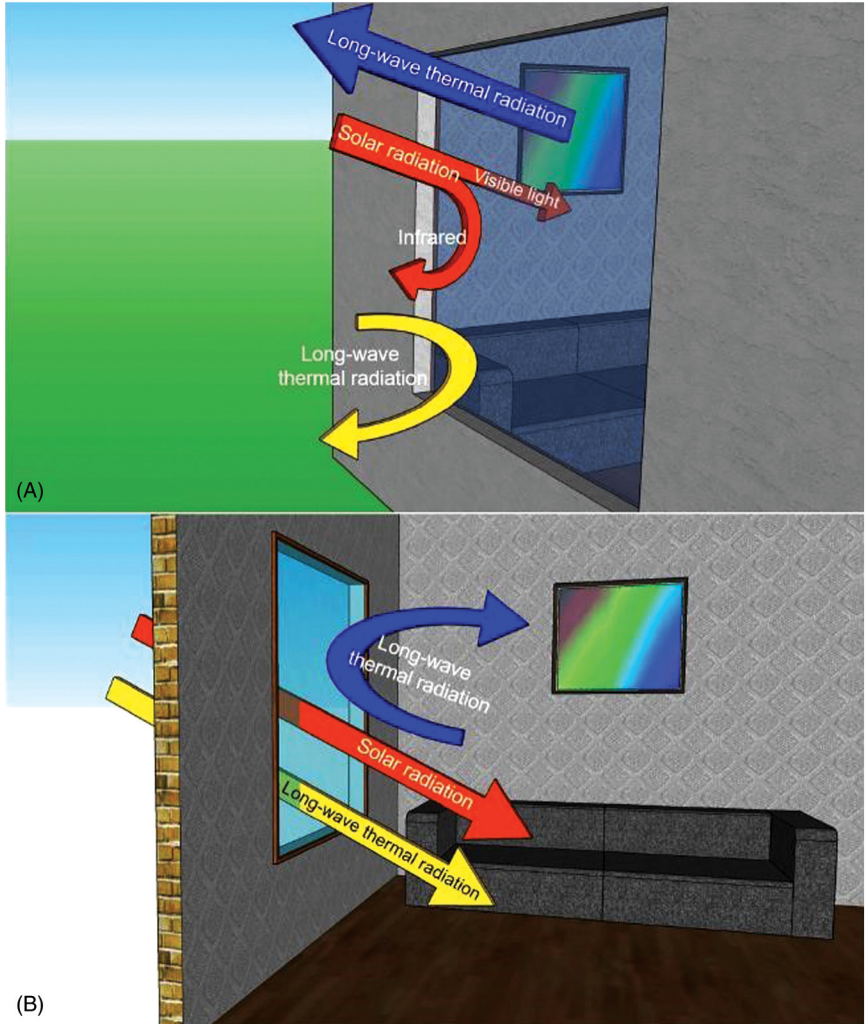


Figure 2.5 *Diagrammatic sketch of perfect windows.* The perfect windows for (A) summer and (B) winter are shown (80).

for surface passivation (88–91). The thin metal layer must have low refractive index in the visible region. The D-M-D multilayered coatings regulate the heat transmission along with the transparency; hence, less energy is consumed in heating and cooling the building. The techniques of growth, structure, and morphology play an important role in regulating the IR radiation. Therefore, materials selectivity play an important role in regulating the heat with visible transparency.

Table 2.3 Spectral properties of perfect windows (80).

Season	Spectral properties	Solar spectrum		Long-wave thermal radiation ($\lambda > 2.5 \mu\text{m}$)	
		Visible light (0.4–0.7 nm)	$\lambda < 0.4 \mu\text{m}$ or $0.7 < \lambda < 2.5 \mu\text{m}$	Outdoor	Indoor
Summer	Spectral transmittance (τ_λ)	100%	0%	0%	100%
	Spectral reflectance (τ_λ)	0%	100%	100%	0%
	Spectral absorptivity (α_λ)	0%	0%	0%	0%
Winter	Spectral transmittance (τ_λ)	100%	100%	100%	0%
	Spectral reflectance (τ_λ)	0%	0%	0%	100%
	Spectral absorptivity (α_λ)	0%	0%	0%	0%

Apart from the optical transparency in the multilayered coatings, durability also plays an important role. The durability to resist from scratches and corrosion from long-term environmental exposure has been reported by Hu et al. (92) by providing the concept of “first durability then reflectivity.” Various transition metals such as Ti, Zr, Hf, V, Nb, Ta, Cr, and Mo were suggested as the durable base, and reflectivity was improved by impinging silver and gold multilayers (92). According to their findings, the traditional mirror coating such as Al/SiO₂ films is best suited for moderate environments; however, Ag-doped HfN film works for harsh environments (Fig. 2.7). In other work by Mishra et al., it is found that Al mirror reflectivity can be enhanced by using multilayers of Al-SiO₂, Al-SiO₂-TiO₂, and Al-Ni-Ag-SiO₂-TiO₂. No change was found in the reflectivity behavior of these multilayers in harsh (accelerated weathering condition and under salt spray with different hours of exposure) conditions (55). The D-M-D-based thin-film encapsulation was designed by Kwon et al. using hybrids of Al₂O₃/Ag/Al₂O₃/S-H (nanocomposite)/Al₂O (93). Here, Al₂O₃ is used as a dielectric layer and Ag as an insertion metal layer. This novel design and technology

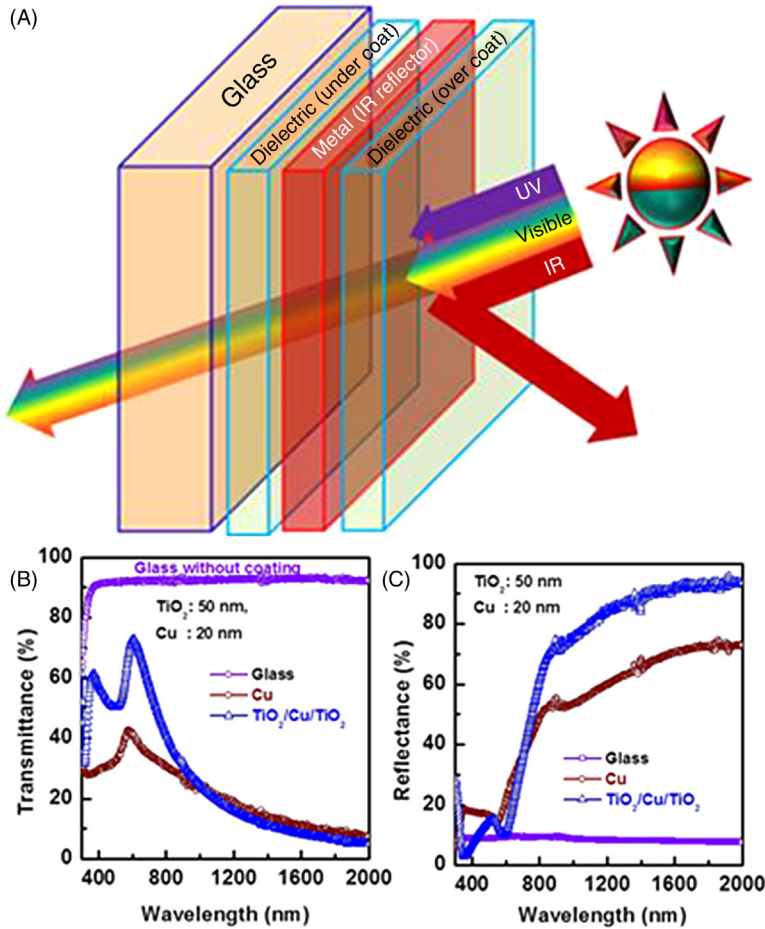


Figure 2.6 (A) Schematic diagram of DMD bases transparent heat mirror. Comparison of optical (B) transmittance and (C) reflectance of glass, thin film Cu (20 nm) and $\text{TiO}_2/\text{Cu}/\text{TiO}_2$ (50 nm/20 nm/50 nm) multilayered thin films without thermal treatment (54,87).

provided the flexible and wearable structure in context of stress relaxation, and heat dissipation (93).

From the above discussion, it is inferred that the growth and micro-structure of the dielectric layer play an important role in the D-M-D-based coatings. Thus, there is need of designing and optimizing the growth parameters and techniques to fabricate the dielectric layers. Apart from the growth of dielectric layer, the selection and thickness of metal layer also play an important role. The thickness of the metal layer affects the optical properties and hence emissivity in I-R coatings. Furthermore, the metal layer should

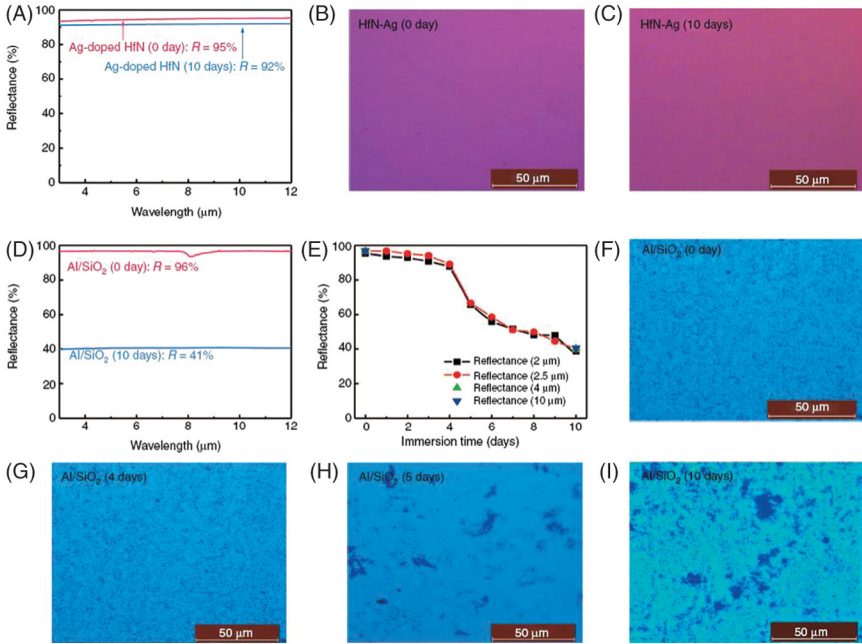


Figure 2.7 (A) The reflectance spectra of the Ag-doped HfN films before/after immersion in a NaCl solution at 35°C for 10 days. Surface of these Ag-doped HfN films (B) before immersion (0 day) and (C) after immersion for 10 days. (D) The reflectance spectra of Al/SiO₂ film before/after immersion in the same NaCl solution for 10 days. (E) Reflectance of the Al/SiO₂ films at various infrared wavelengths (2, 2.5, 4, and 10 μm) as a function of the immersion time. Typical surface of Al/SiO₂ films (F) before immersion (0 day), (G) after immersion for 4 days, (H) 5 days, and (I) 10 days (92).

be chosen so that the interdiffusion of the metal layer is avoided during deposition and hence the stability gets enhanced (94). Thus, the optimization of metal layer thickness is also an important factor in D-M-D-based I-R coatings.

5.2 Thermo-chromic materials and coatings

These are the materials whose optical properties are varied as a function of temperature. The properties of the materials are changed upon heating and while cooling, the material returns to its original state. The change in optical properties on heating and cooling is related to the change in the phase structure of the material. The transmittance and reflectance are modified due to phase transition. This change in phase, and hence optical properties of a material by heating and cooling, results in generation of the color, hence the name thermo-chromic (T-C) materials.

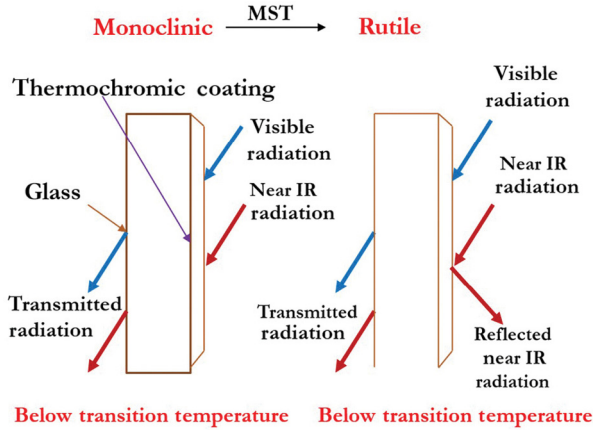


Figure 2.8 Schematic representation of thermochromic materials applied as an intelligent windows coating (84,99).

The T-C materials play an important role in reducing the energy consumption and target toward lowering future energy demands. The T-C materials optimize the optical properties of a material and reduce the unwanted solar energy gain (80,87,95,96). There are various materials that are used for T-C coating. However, vanadium dioxide (VO_2) proves to be an ideal material for such coatings. VO_2 is initially at monoclinic state. The monoclinic state changes to rutile at 68°C . This phase change with the change in temperature shows the reversible metal to semiconductor phase transition (81,86,87), see Fig. 2.8. The change in phase with temperature of VO_2 leads to stupendous optical properties (81). At low temperature (below transition temperature), VO_2 is in insulating state and allows transmission of the visible and IR. As the temperature rises above transition temperature, the VO_2 film is converted to metallic phase that allows visible light but blocks IR (87,98). This transition of phase with temperature allows VO_2 to be a T-C material for smart windows application.

Yang et al., in their studies, show the integration of thermochromic VO_2 on flexible substrates forming hybridized VO_2 /graphene, see Fig. 2.9. These T-C coating-based smart windows may respond to environmental temperatures to regulate light transmittance (86).

In order to modify the optical properties of VO_2 for smart window applications, it is doped with various metals (87,98). Doping with metals changes the transition temperature of VO_2 films (87). Tungsten (W) has proven to be a wonderful metal for doping as it reduces the transition temperature VO_2 to 25°C by 2% doping (98). Apart from W, gold (Au) and fluorine have also been reported to be used as dopant materials (84).

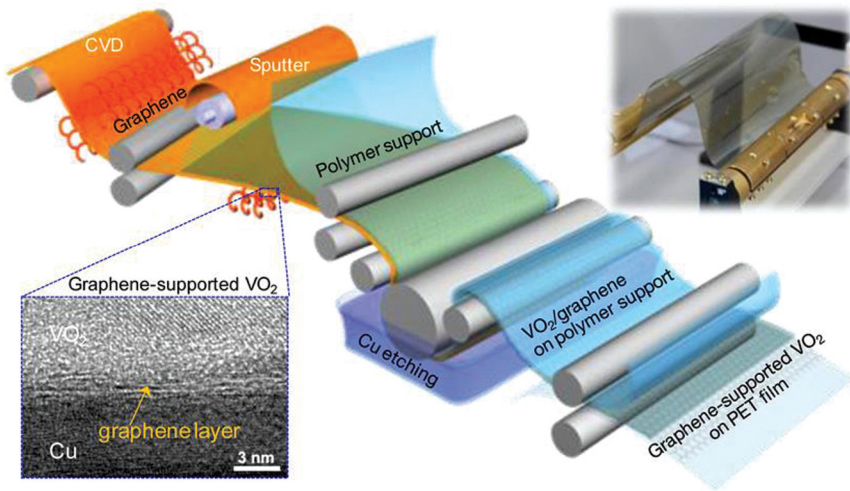


Figure 2.9 Schematic representation of thermochromic hybridized $\text{VO}_2/\text{graphene}$ (86).

6 Conclusions

The interaction of IR radiation with various materials for different coatings is discussed in this chapter. It is inferred that multilayer coatings play an important role in energy-efficient smart window applications by variation in their optical properties. The wavelengths at which different optical coatings (thin films/nanostructures) perform vary over a wide range of wavelengths. Different materials coatings, such as dielectric-metal-dielectric (D-M-D) and thermo-chromic (T-C) are discussed. The chapter discusses in brief about the selection of materials, synthesis techniques, for the different IR coatings.

References

1. Diffey, B. L. Sources and Measurement of Ultraviolet Radiation. *Methods* **2002**, *28* (1), 4–13.
2. Grenfell, T. C.; Warren, S. G.; Mullen, P. C. Reflection of Solar Radiation by the Antarctic Snow Surface at Ultraviolet, Visible, and Near-Infrared Wavelengths. *J. Geophys. Res. Atmos.* **1994**, *99* (D9), 18669–18684.
3. Bitran M.; Murray W. Infrared, Visible, and Ultraviolet Radiation. In *E. Bingham, B. Cohnsen and C. Powell, Eds., Patty's Toxicology*; John Wiley & Sons, Inc., New York, **2001**, 249–314.
4. Wang, J., et al. Recent Progress on Localized Field Enhanced Two-Dimensional Material Photodetectors from Ultraviolet—Visible to Infrared. *Small* **2017**, *13* (35), 1700894.
5. Ring, E. F. J. The Discovery of Infrared Radiation in 1800. *Imaging Sci. J.* **2000**, *48* (1), 1–8.

6. Manley, M.; Baeten, V. Chapter 3—Spectroscopic Technique: Near Infrared (NIR) Spectroscopy. In Da-Wen Sun, 2nd ed.; *Modern Techniques for Food Authentication* pp. 51–102.
7. Dwivedi, B. James Clerk Maxwell and His Equations. *Resonance* **2003**, *8*, 4–16.
8. Tian, L., et al. Broad Range Energy Absorption Enabled by Hydrogenated TiO₂ Nanosheets: From Optical to Infrared and Microwave. *J. Mater. Chem. C* **2017**, *5* (19), 4645–4653.
9. Fang, V., et al., A Review of Near Infrared Reflectance Properties of Metal Oxide Nanostructures. GNS Science Report, 2013.
10. Caplan, J. D., et al. Near-Infrared Spectroscopy for the Detection of Vulnerable Coronary Artery Plaques. *J. Am. Coll. Cardiol.* **2006**, *47* (8 Suppl.), C92–C96.
11. Feng, R., et al. Visible- and NIR-Light Responsive Black-Phosphorus-Based Nanostructures in Solar Fuel Production and Environmental Remediation. *Adv. Mater.* **2018**, *30*, 1804770.
12. Alibabaei, L.; Brennaman, M. K.; Meyer, T. J. Light-Driven Water Splitting in the Dye-Sensitized Photoelectrosynthesis Cell. In H. Tian, G. Boschloo and A. Hagfeldt, *Molecular Devices for Solar Energy Conversion and Storage*; Springer, **2018**, 229–257.
13. Fujishima, A.; Honda, K. Electrochemical Photolysis of Water at a Semiconductor Electrode. *Nature* **1972**, *238* (5358), 37.
14. Fung, C. K. M., et al. Nanoresonant Signal Boosters for Carbon Nanotube Based Infrared Detectors. *Nanotechnology* **2009**, *20* (18), 185201.
15. Grätzel, M. Recent Advances in Sensitized Mesoscopic Solar Cells. *Acc. Chem. Res.* **2009**, *42* (11), 1788–1798.
16. Kastek, M., et al. Test Bed for Measurement of Angular Parameters of Passive Infrared Sensors. *Infrared Phys. Technol.* **2007**, *49* (3), 198–201.
17. Matsui, T., et al. A Novel Method to Prevent Secondary Exposure of Medical and Rescue Personnel to Toxic Materials Under Biochemical Hazard Conditions Using Microwave Radar and Infrared Thermography. *IEEE Trans. Biomed. Eng.* **2004**, *51* (12), 2184–2188.
18. Rogalski, A. *Infrared detectors* CRC Press: Boca Raton, FL, 2011.
19. Yu, P. Y.; Cardona, M. *Fundamentals of Semiconductors: Physics and Materials Properties*. Springer, 1996.
20. Chen, X., et al. Semiconductor-Based Photocatalytic Hydrogen Generation. *Chem. Rev.* **2010**, *110* (11), 6503–6570.
21. Chen, X., et al. Nanomaterials for Renewable Energy Production and Storage. *Chem. Soc. Rev.* **2012**, *41* (23), 7909–7937.
22. Vollmer, M.; Möllmann, K. -P. *Infrared Thermal Imaging: Fundamentals, Research and Applications Wiley-VCH; 2 edition*.
23. Gupta, R. P. *Remote sensing geology*. Springer-Verlag, 2017.
24. Kocer, H., et al. Reduced Near-Infrared Absorption Using Ultra-Thin Lossy Metals in Fabry-Perot Cavities. *Sci. Rep.* **2015**, *5*, 8157.
25. Bergström, D. *The Absorption of Laser Light by Rough Metal Surfaces*. Luleå tekniska universitet, 2008.
26. Subasri, A., et al. Economical Development of IR Coatings in Asbestos Sheet. *Int. J. Curr. Res. Life Sci.* **2018**, *7* (5), 2062–2066.
27. Nilsson, C. and T. Halberg, (2001) Multilayer structures for low emissive paint, Sensor Technology.
28. Hu, T., et al. Correlation Between Reflectivity and Resistivity in Multi-Component Metallic Systems. *Appl. Phys. Lett.* **2012**, *101* (1), 011902.
29. Faulkner, E. B.; Schwartz, R. J. *High Performance Pigments*. John Wiley & Sons, 2009.
30. Nayfeh, M. H. Optics in Nanotechnology. In M. D. Al-Amri, Mohamed El-Gomati, M. S. Zubairy, *Optics in Our Time*; Springer, **2016**, pp. 223–264.
31. Dong, L. *Optical Properties of Nanoparticles in Composite Materials*. KTH Royal Institute of Technology, 2012.

32. Rugh, J. P., et al. *Reduction in Vehicle Temperatures and Fuel Use From Cabin Ventilation, Solar-Reflective Paint, and a New Solar-Reflective Glazing*. SAE Technical Paper.
33. Brady, R. F., Jr.; Wake, L.V. Principles and Formulations for Organic Coatings with Tailored Infrared Properties. *Prog. Org. Coat.* **1992**, *20*, 1–25.
34. Kumar, S.; Verma, N. K.; Singla, M. L. Study on Reflectivity and Photostability of Al-doped TiO₂ Nanoparticles and Their Reflectors. *J. Mater. Res.* **2013**, *28* (3), 521–528.
35. Ranade, A. *Synthesis and Characterization of Transparent Oxide Coatings with Enhanced Near Infrared Reflectance*. Northwestern University, 2011.
36. Fangli, Y., et al. Preparation and Properties of Zinc Oxide Nanoparticles Coated with Zinc Aluminate. *J. Mater. Chem.* **2003**, *13* (3), 634–637.
37. Bendiganavale, A.; Malshe, V. *Infrared Reflective Inorganic Pigments* **2010**, 1.
38. Haacke, G. Transparent Electrode Properties of Cadmium Stannate. *Appl. Phys. Lett.* **1976**, *28*, 622.
39. Zheng, B., et al. Identifying Key Factors Towards Highly Reflective Silver Coatings. *Adv. Mater. Sci. Eng.* **2017**, *2017*, 12.
40. Jung, K. T.; Shul, Y. G. Preparation of Transparent TS-1 Zeolite Film by Using Nanosized TS-1 Particles. *Chem. Mater.* **1997**, *9* (2), 420–422.
41. Lagorio, M. G. Why Do Marbles Become Paler on Grinding? Reflectance, Spectroscopy, Color, and Particle Size. *J. Chem. Educ.* **2004**, *81* (11), 1607.
42. Rocquefelte, X., et al. Investigation of the Origin of the Empirical Relationship between Refractive Index and Density on the Basis of First Principles Calculations for the Refractive Indices of Various TiO₂ Phases. *Inorg. Chem.* **2004**, *43* (7), 2246–2251.
43. Malshe, V. C.; Bendiganavale, A. K. Infrared Reflective Inorganic Pigments. *Recent Patents Chem. Eng.* **2008**, *1* (1), 67–79.
44. Wang, P., et al. Effect of Silicon Carbide Ceramic Coating Process on the Mirror Surface Quality. Eighth International Symposium on Advanced Optical Manufacturing and Testing Technology (AOMATT2016).
45. Jeevanandam, P., et al. Near Infrared Reflectance Properties of Metal Oxide Nanoparticles. *J. Phys. Chem. C* **2007**, *111* (5), 1912–1918.
46. Shrestha, K. M.; Sorensen, C. M.; Klabunde, K. J. Synthesis of CuO Nanorods, Reduction of CuO into Cu Nanorods, and Diffuse Reflectance Measurements of CuO and Cu Nanomaterials in the Near Infrared Region. *J. Phys. Chem. C* **2010**, *114* (34), 14368–14376.
47. Li, Y. -Q., et al. Highly Solar Radiation Reflective Cr₂O₃·3TiO₂ Orange Nanopigment Prepared by a Polymer-Pyrolysis Method. *ACS Sustain. Chem. Eng.* **2014**, *2* (2), 318–321.
48. Nikolic, N. D.; Rakočević, Z.; Popov, K. I. Reflection and Structural Analyses of Mirror-Bright Metal Coatings. *J. Solid State Electrochem.* **2004**, *8* (8), 526–531.
49. Goossens, V., et al. Predicting Reflections of Thin Coatings. *Surf. Coat. Technol.* **2009**, *204* (5), 551–557.
50. Lee, C. -C.; Chen, S. -H.; Jaing, C. -C. Optical Monitoring of Silver-Based Transparent Heat Mirrors. *Appl. Opt.* **1996**, *35* (28), 5698–5703.
51. Yoldas, B. E.; O'Keefe, T. Deposition of Optically Transparent IR Reflective Coatings on Glass. *Appl. Opt.* **1984**, *23* (20), 3638–3643.
52. Woong-Sun, Y., et al. Ag/Ni/Ag Multilayer Reflector for GaN-Based Vertical Light-Emitting Diode. *Jpn J. Appl. Phys.* **2013**, *52* (5R), 052101.
53. Martín-Palma, R. J., et al. In-Depth Optical and Structural Study of Silver-Based Low-Emissivity Multilayer Coatings for Energy-Saving Applications. *J. Phys. D* **2004**, *37* (11), 1554.
54. Dalapati, G. K., et al. Color Tunable Low Cost Transparent Heat Reflector Using Copper and Titanium Oxide for Energy Saving Application. *Sci. Rep.* **2016**, *6*, 20182.
55. Mishra, S. K., et al. Development and Degradation Behavior of Protective Multilayer Coatings for Aluminum Reflectors for Solar Thermal Applications. *Thin Solid Films* **2016**, *619*, 202–207.

56. Kure-Chu, S., et al. Multilayered Sn/Ag₃Sn electroplating on Cu alloys for high reliable electronic/electric materials. 2014 International Conference on Electronics Packaging (ICEP).
57. Wang, X., et al. Thermal Annealing Effect on Optical Properties of Binary TiO₂-SiO₂ Sol-Gel Coatings. *Materials (Basel, Switzerland)* **2012**, *6* (1), 76–84.
58. Liu, Y. Y., et al. Natural Superhydrophilic TiO₂/SiO₂ Composite Thin Films Deposited by Radio Frequency Magnetron Sputtering. *J. Alloys Compounds* **2009**, *479* (1), 532–535.
59. Hodroj, A., et al. Thermal Annealing of Amorphous Ti-Si-O Thin Films. *J. Mater. Res.* **2011**, *23* (3), 755–759.
60. Nilchi, A., et al. New TiO₂/SiO₂ Nanocomposites—Phase Transformations and Photocatalytic Studies. *Colloids Surf. A* **2010**, *361* (1), 25–30.
61. Liu, X., et al. CaF₂:Ce³⁺/Yb³⁺ Hollow Spheres Luminescence Downconversion Property Optimize Anti-Reflective Coatings for Solar Cells. *Solar Energy* **2016**, *134*, 45–51.
62. Pedroni, M., et al. Water (H₂O and D₂O) Dispersible NIR-to-NIR Upconverting Yb³⁺/Tm³⁺ Doped MF₂ (M = Ca, Sr) Colloids: Influence of the Host Crystal. *Cryst. Growth Des.* **2013**, *13* (11), 4906–4913.
63. Baetens, R.; Jelle, B. P.; Gustavsen, A. Properties, Requirements and Possibilities of Smart Windows for Dynamic Daylight and Solar Energy Control in Buildings: A State-of-the-art Review. *Sol. Energy Mater. Sol. Cells* **2010**, *94* (2), 87–105.
64. Shi, Y., et al. Crystal Structure and Near-Infrared Reflective Properties of Fe³⁺ Doped AlPO₄ Pigments. *Ceram. Int.* **2017**, *43* (8), 5979–5983.
65. Yang, R., et al. Synthesis, Characterization and Thermal Performance of Fe/N co-doped MgTiO₃ as a Novel High Near-Infrared Reflective Pigment. *Sol. Energy Mater. Sol. Cells* **2017**, *160*, 307–318.
66. George, G.; Vishnu, V. S.; Reddy, M. L. P. The Synthesis, Characterization and Optical Properties of Silicon and Praseodymium Doped Y₆MoO₁₂ Compounds: Environmentally Benign Inorganic Pigments with High NIR Reflectance. *Dyes Pigments* **2011**, *88* (1), 109–115.
67. Sorokin, O., et al. Joining of Silicon Carbide Ceramic by Hybrid Spark Plasma Sintering. *Russ. J. Appl. Chem.* **2015**, *88*, 839–845.
68. Komarevskiy, N., et al. Potential of Glassy Carbon and Silicon Carbide Photonic Structures as Electromagnetic Radiation Shields for Atmospheric Re-entry. *Opt. Express* **2012**, *20*, 14189–14200.
69. Bilokur, M., et al. Optical Properties of Refractory TiN, AlN and (Ti,Al)N Coatings. SPIE Micro+Nano Materials, Devices, and Applications, SPIE.
70. Thirugnanambantham, K. G.; Natarajan, S. Degradation Mechanism for High Temperature Erosion in Surface Modified IN718 Superalloy. *Surf. Eng.* **2015**, *31* (1), 24–28.
71. Chen, W., et al. Thiophene-Fused-Heteroaromatic Diones as Promising NIR Reflectors for Radiative Cooling. *Angew. Chem. Int. Ed.* **2018**, *57* (21), 6289–6293.
72. Lin, Y.; Li, Y.; Zhan, X. Small Molecule Semiconductors for High-Efficiency Organic Photovoltaics. *Chem. Soc. Rev.* **2012**, *41* (11), 4245–4272.
73. Kaur, B.; Bhattacharya, S. N.; Henry, D. J. Interpreting the Near-Infrared Reflectance of a Series of Perylene Pigments. *Dyes Pigm.* **2013**, *99* (2), 502–511.
74. Lampert, C. M. Chromogenic Smart Materials. *Mater. Today* **2004**, *7* (3), 28–35.
75. Lampert, C. M. Large-Area Smart Glass and Integrated Photovoltaics. *Sol. Energy Mater. Sol. Cells* **2003**, *76* (4), 489–499.
76. Lechner, R.; Thomas, L. K. All Solid State Electrochromic Devices on Glass and Polymeric Foils. *Sol. Energy Mater. Sol. Cells* **1998**, *54* (1), 139–146.
77. Hu, X., et al. Effective Electrically Tunable Infrared Reflectors Based on Polymer Stabilised Cholesteric Liquid Crystals. *Liquid Cryst.* **2018**, *46*, 1–8.

78. Khandelwal, H., et al. Electrically Switchable Polymer Stabilised Broadband Infrared Reflectors and Their Potential as Smart Windows for Energy Saving in Buildings. *Sci. Rep.* **2015**, *5*, 11773.
79. Chen, X., et al. Broadband Reflection of Polymer-Stabilized Chiral Nematic Liquid Crystals Induced by a Chiral Azobenzene Compound. *Chem. Commun.* **2014**, *50* (6), 691–694.
80. Long, L.; Ye, H. How to be Smart and Energy Efficient: A General Discussion on Thermochromic Windows. *Sci. Rep.* **2014**, *4*, 6427.
81. Gao, Y., et al. Nanoceramic VO₂ Thermochromic Smart Glass: A Review on Progress in Solution Processing. *Nano Energy* **2012**, *1* (2), 221–246.
82. Al-Shukri, A. M. Thin Film Coated Energy-Efficient Glass Windows for Warm Climates. *Desalination* **2007**, *209* (1), 290–297.
83. Sadineni, S. B.; Madala, S.; Boehm, R. F. Passive Building Energy Savings: A Review of Building Envelope Components. *Renew. Sust. Energy Rev.* **2011**, *15* (8), 3617–3631.
84. Kamalisarvestani, M., et al. Performance, Materials and Coating Technologies of Thermochromic Thin Films on Smart Windows. *Renew. Sust. Energy Rev.* **2013**, *26*, 353–364.
85. Fan, J. C. C., et al. Transparent Heat-Mirror Films of TiO₂/Ag/TiO₂ for Solar Energy Collection and Radiation Insulation. *Appl. Phys. Lett.* **1974**, *25* (12), 693–695.
86. Kim, H., et al. Flexible Thermochromic Window Based on Hybridized VO₂/Graphene. *ACS Nano* **2013**, *7* (7), 5769–5776.
87. Dalapati, G. K., et al. Transparent Heat Regulating (THR) Materials and Coatings for Energy Saving Window Applications: Impact of Materials Design, Micro-Structural, and Interface Quality on the THR Performance. *Prog. Mater. Sci.* **2018**, *95*, 42–131.
88. Dan, A., et al. Solar Energy Absorption Mediated by Surface Plasma Polaritons in Spectrally Selective Dielectric-Metal-Dielectric Coatings: A Critical Review. *Renew. Sust. Energy Rev.* **2017**, *79*, 1050–1077.
89. Al-Kuhaili, M. F., et al. Energy-Saving Transparent Heat Mirrors Based on Tungsten Oxide–Gold WO₃/Au/WO₃ Multilayer Structures. *Sol. Energy* **2012**, *86* (11), 3183–3189.
90. Kulczyk–Malecka, J., et al. Investigation of Silver Diffusion in TiO₂/Ag/TiO₂ Coatings. *Acta Mater.* **2013**, *66*, 396.
91. Peres, L. ZnS|Ag|TiO₂ multilayer electrodes with broadband transparency for thin film solar cells. *RSC Adv.* **2016**, *6* (66), 61057–61063.
92. Hu, C., et al. New Design for Highly Durable Infrared-Reflective Coatings. *Light Sci. Appl.* **2018**, *7*, 17175.
93. Kwon, J. H., et al. Functional Design of Dielectric-Metal-Dielectric-Based Thin-Film Encapsulation with Heat Transfer and Flexibility for Flexible Displays. *ACS Appl. Mater. Interfaces* **2017**, *9*, 27062–27072.
94. Sharma, H.; Shukla, A. K.; Vankar, V. D. Effect of Titanium Interlayer on the Microstructure and Electron Emission Characteristics of Multiwalled Carbon Nanotubes. *J. Appl. Phys.* **2011**, *110* (3), 033726.
95. Greenberg, C. B. Undoped and Doped VO₂ Films Grown From VO(OC₃H₇)₃. *Thin Solid Films* **1983**, *110* (1), 73–82.
96. Parkin, I. P.; Manning, T. D. Intelligent Thermochromic Windows. *J. Chem. Educ.* **2006**, *83* (3), 393.
97. Blackman, C. S., et al. Atmospheric Pressure Chemical Vapour Deposition of Thermochromic Tungsten Doped Vanadium Dioxide Thin Films for Use in Architectural Glazing. *Thin Solid Films* **2009**, *517* (16), 4565–4570.
98. Wu, C.; Feng, F.; Xie, Y. Design of Vanadium Oxide Structures with Controllable Electrical Properties for Energy Applications. *Chem. Soc. Rev.* **2013**, *42* (12), 5157–5183.
99. Kiri, P.; Hyett, G.; Binions, R. Solid State Thermochromic Materials. *Adv. Mater. Lett.* **2010**, *1*, 86–105.